Microtubule-dependent redistribution of the type-1 inositol 1,4,5-trisphosphate receptor in A7r5 smooth muscle cells

Elke Vermassen[1], Kristel Van Acker[1], Wim G. Annaert[2], Bernard Himpens[1], Geert Callewaert[1], Ludwig Missiaen[1], Humbert De Smedt[1] and Jan B. Parys[1,*]

[1]Laboratory of Physiology and [2]Laboratory for Neuronal Membrane Trafficking, CME/VIB04, K.U. Leuven Campus Gasthuisberg O/N, Herestraat 49, B-3000 Leuven, Belgium

*Author for correspondence (e-mail: Jan.Parys@med.kuleuven.ac.be)

Accepted 7 January 2003
Journal of Cell Science 116, 1269-1277 © 2003 The Company of Biologists Ltd
doi:10.1242/jcs.00354

Summary

In A7r5 vascular smooth muscle cells, the two expressed inositol 1,4,5-trisphosphate receptor (IP_3R) isoforms were differentially localized. IP_3R1 was predominantly localized in the perinuclear region, whereas IP_3R3 was homogeneously distributed over the cytoplasm. Prolonged stimulation (1-5 hours) of cells with 3 μM arginine-vasopressin induced a redistribution of IP_3R1 from the perinuclear region to the entire cytoplasm, whereas the localization of IP_3R3 appeared to be unaffected. The redistribution process occurred independently of IP_3R downregulation. No structural changes of the endoplasmic reticulum were observed, but SERCA-type Ca^{2+} pumps redistributed similarly to IP_3R1. The change in IP_3R1 localization induced by arginine-vasopressin could be blocked by the simultaneous addition of nocodazole or taxol and depended on Ca^{2+} release from intracellular stores since Ca^{2+}-mobilizing agents such as thapsigargin and cyclopiazonic acid could induce the redistribution. Furthermore, various protein kinase C inhibitors could inhibit the redistribution of IP_3R1, whereas the protein kinase C activator 1-oleoyl-2-acetyl-sn-glycerol induced the redistribution. Activation of protein kinase C also induced an outgrowth of the microtubules from the perinuclear region into the cytoplasm, similar to what was seen for the redistribution of IP_3R1. Finally, blocking vesicular transport at the level of the intermediate compartment inhibited the redistribution. Taken together, these findings suggest a role for protein kinase C and microtubuli in the redistribution of IP_3R1, which probably occurs via a mechanism of vesicular trafficking.

Key words: Calcium stores, Calcium, Cytoskeleton, Protein kinase C, Intracellular calcium channel

Introduction

Cellular activation by many agonists results in the stimulation of phospholipase C (PLC) and the subsequent hydrolysis of phosphatidylinositol 4,5-bisphosphate to inositol 1,4,5-trisphosphate (IP_3) and diacylglycerol (DAG) (Berridge, 1993). Each of these two molecules exerts a specific effect in the cell. The increased DAG concentration leads to the activation of protein kinase C (PKC) while IP_3 binds to the IP_3 receptor (IP_3R), an intracellular Ca^{2+}-release channel located in the endoplasmic reticulum (ER), thereby inducing Ca^{2+} release from internal stores. A prolonged stimulation of cells with agonists, however, results in downregulation of the IP_3Rs and this appears to be a cell- and agonist-specific process (Sipma et al., 1998; Wojcikiewicz, 1995). This downregulation results from an accelerated IP_3R degradation (Wojcikiewicz et al., 1994) and is mediated by the ubiquitin-proteasome pathway (Oberdorf et al., 1999).

Ca^{2+} signals evoked by agonist stimulation have complex temporal and spatial characteristics, and the underlying mechanisms are not yet fully understood (Berridge et al., 1998). The differential regulation of the IP_3R isoforms by various modulators of IP_3-induced Ca^{2+} release, such as IP_3, cytosolic Ca^{2+}, ATP, calmodulin and phosphorylation by several kinases, may contribute to this intricate pattern (Patel et al., 1999). There is evidence that global responses, such as Ca^{2+} waves and oscillations, are generated by the recruitment of a threshold number of Ca^{2+} puffs (Bootman and Berridge, 1995; Marchant and Parker, 2001; Van Acker et al., 2000). Ca^{2+} puffs themselves can provide highly localized signals leading to activation of specific phenomena such as muscle relaxation in smooth muscle cells (Nelson et al., 1995). The intracellular localization of the Ca^{2+} channels plays an important role in these processes because the subcellular distribution of the puff sites determines the spatial pattern of the Ca^{2+} signals.

The distribution of IP_3Rs is dependent on isoform and cell type as recently shown in, for example, pancreatic and salivary gland cells (Lee et al., 1997; Zhang et al., 1999), oocytes (Fissore et al., 1999), aortic smooth muscle cells (Tasker et al., 2000) and aortic endothelial, adrenal glomerulosa and COS-7 cells (Laflamme et al., 2002). Differences in properties and distribution of IP_3R isoforms can therefore determine the cell-specific pattern of the Ca^{2+} signals (Hirata et al., 1999). Moreover, a particular isoform can have multiple locations in a cell. In myotubes of cultured mouse muscle, for example, IP_3R1 is localized in both the perinuclear region and at the I band of the sarcoplasmic reticulum (Powell et al., 2001).

Finally, the localization of IP_3Rs can change in response to Ca^{2+} elevations (Wilson et al., 1998). In RBL-2H3 cells, IP_3R2 forms large clusters after treatment with Ca^{2+}-mobilizing agents. This redistribution required a sustained Ca^{2+} influx, but the precise mechanism is not yet understood. An increase in cytosolic Ca^{2+} concentration can also affect ER structure (Subramanian and Meyer, 1997; Wilson et al., 1998).

Cytoskeletal elements, such as microtubuli and microfilaments, can also contribute to the maintenance of local Ca^{2+} spikes and can determine the position of the Ca^{2+}-release apparatus via a local organization of the ER (Fogarty et al., 2000). Furthermore, the cytoskeleton can change rapidly in response to extracellular signals (Keenan and Kelleher, 1998). PKC, which is activated after agonist stimulation (Nishizuka, 1988), has recently been found to have a substantial effect on the microtubules. In neuronal growth cones, activation of PKC resulted in a rapid growth of the microtubules (Kabir et al., 2001).

In this study, we investigated the intracellular localization of IP_3R1 and IP_3R3 in A7r5 vascular smooth muscle cells. A7r5 cells have been used as a model system for studying IP_3R1 function (Missiaen et al., 1996; Missiaen et al., 1998). It also was recently found that IP_3-induced Ca^{2+} release, capacitative Ca^{2+} entry and proliferation in A7r5 cells predominantly depended on the type 1 isoform (Wang et al., 2001). We found that IP_3R1 and IP_3R3 were differently localized in these cells. Moreover, after prolonged agonist stimulation, an intracellular redistribution of IP_3R1 but not of IP_3R3 was observed. This redistribution was dependent on PKC activation and the integrity of the microtubular network, and occurs most probably via vesicle trafficking.

Materials and Methods

Materials

Imipramine, [Arg^8]-vasopressin (AVP), thapsigargin, staurosporine, nocodazole, bisindolylmaleimide I hydrochloride, 1-oleoyl-2-acetyl-sn-glycerol (OAG), cyclopiazonic acid (CPA), taxol, brefeldin A, Triton X-100 and goat serum were from Sigma (St Louis, MO). MG-132 and Gö-6976 were from Calbiochem-Novabiochem (San Diego, CA). Rhodamine-phalloidin was obtained from Molecular Probes (Eugene, OR). IP_3BM was a kind gift from M. D. Bootman (Babraham, UK).

Cell culture

A7r5 (ATCC CRL 1444) is an established cell line derived from embryonic rat aorta. These smooth muscle cells were grown in 9% CO_2 at 37°C in Dulbecco's modified Eagle medium supplemented with 10% fetal calf serum, 0.9% (v/v) non-essential amino acids, 3.8 mM L-glutamine, 85 IU/ml penicillin and 85 μg/ml streptomycin.

Transfection

For transfection experiments, cells were seeded in two-well chambered coverglasses (Nunc, Naperville, IL) at a density of 6000 cells/cm^2. After 48 hours, cells were transfected with 0.85 μg pEYFP-ER vector DNA, coding for an ER-targeted enhanced yellow fluorescent protein (EYFP) (Clontech Laboratories, Palo Alto, CA) and 3.4 μl of Fugene™ transfection reagent (Roche Diagnostics, Mannheim, Germany).

Antibodies

Immunolocalization of IP_3R1 was performed with the previously characterized antibodies Rbt03 and Rbt04 directed against the C-terminus of IP_3R1 (Parys et al., 1995), as well as with the anti-loopI17a-2 antibody against the luminal Ca^{2+}-binding site (Maes et al., 2001), the anti-cytI3b-1 antibody against the Ca^{2+}-binding domain 3b localized in the IP_3-binding domain (Sipma et al., 1999), and an affinity-purified antibody directed against amino acids 1829-1848 (Affinity BioReagents, Golden, CO).

IP_3R3 was localized with the monoclonal antibody MMAtype 3, obtained from Transduction Laboratories (Lexington, KY), that recognizes the N-terminal region of IP_3R3 (De Smedt et al., 1997).

Protein disulfide isomerase (PDI) and BiP were visualized with monoclonal antibodies raised against purified rat PDI (Affinity BioReagents, Golden, CO) and the C-terminus of human BiP (Transduction Laboratories, Lexington, KY), respectively. Sarco(endo)plasmic reticulum Ca^{2+}-ATPase (SERCA) was localized using the AS809-27 polyclonal antibody directed against amino acids 809-827 of SERCA1a that recognizes all SERCA isoforms (Møller et al., 1997).

The anti-α-tubulin monoclonal antibody (Sigma), raised against an epitope located in the C-terminal end of α-tubulin, was used to detect the microtubular network. Fluorescein isothiocyanate (FITC)-conjugated secondary goat anti-mouse and goat anti-rabbit antibodies were from Sigma.

Immunofluorescence of IP_3R1 and IP_3R3

For confocal microscopy, A7r5 cells were seeded at a density of 8000 cells/cm^2 in two-well chambered coverglasses. Stimulation with the various reagents occurred at 37°C in Ca^{2+}- and Mg^{2+}-free Dulbecco's phosphate-buffered saline (PBS) for the times indicated in the legends of the figures, unless otherwise indicated. Control cells were incubated accordingly in PBS. After incubation, cells were fixed in 3% paraformaldehyde in PBS for 15 minutes at room temperature. After permeabilization with 0.5% Triton X-100 in PBS for 5 minutes, cells were washed three times in PBS. Non-specific binding sites were blocked with 20% goat serum in PBS for 1 hour before incubation with the primary antibodies, which were diluted in PBS containing 1.5% goat serum. Subsequently, cells were washed three times with PBS and incubated with the FITC-conjugated anti-rabbit or anti-mouse secondary antibody. As a control, cells were treated as above but incubated with either the pre-immune serum of Rbt03 or with PBS before secondary antibodies were added. The coverglasses were examined using a Zeiss confocal laser scanning microscope LSM 510 (CLSM) (Carl Zeiss, Jena, Germany) with a Plan-Neofluar® 40× numerical aperture 1.3 oil-immersion objective. FITC was excited at 488 nm using an argon laser and fluorescent light was collected by a photomultiplier after passage through a 505 nm LP filter. For statistical analysis, random fields were chosen and cells were counted. A minimum of 100 cells was counted in each independent experiment. Depending on the localization of IP_3R1, two cell types were discerned: (a) cells with IP_3R1 in a preferentially perinuclear localization, and (b) cells with a homogeneous distribution of IP_3R1. When cells could not clearly be assigned to one of these two categories, they were classified into a third group, which is referred to as the intermediate state. The intermediate cell type always amounted to less than 11% of the total number of cells.

When indicated, 18 slices throughout the entire cell, with an interval of 0.5 μm between each slice, were used to generate a Z-stack. Each of the images of the Z-stack was superimposed over the previous one to generate a flattened Z-stack.

Visualization of ER and cytoskeleton

For immunolocalization experiments, cells were treated as above, using anti-BiP (1/500), anti-PDI (1/100) and AS809-27 (1/300) for the detection of the various ER proteins. The ER was also visualized after heterologous expression of ER-targeted EYFP. Coverglasses

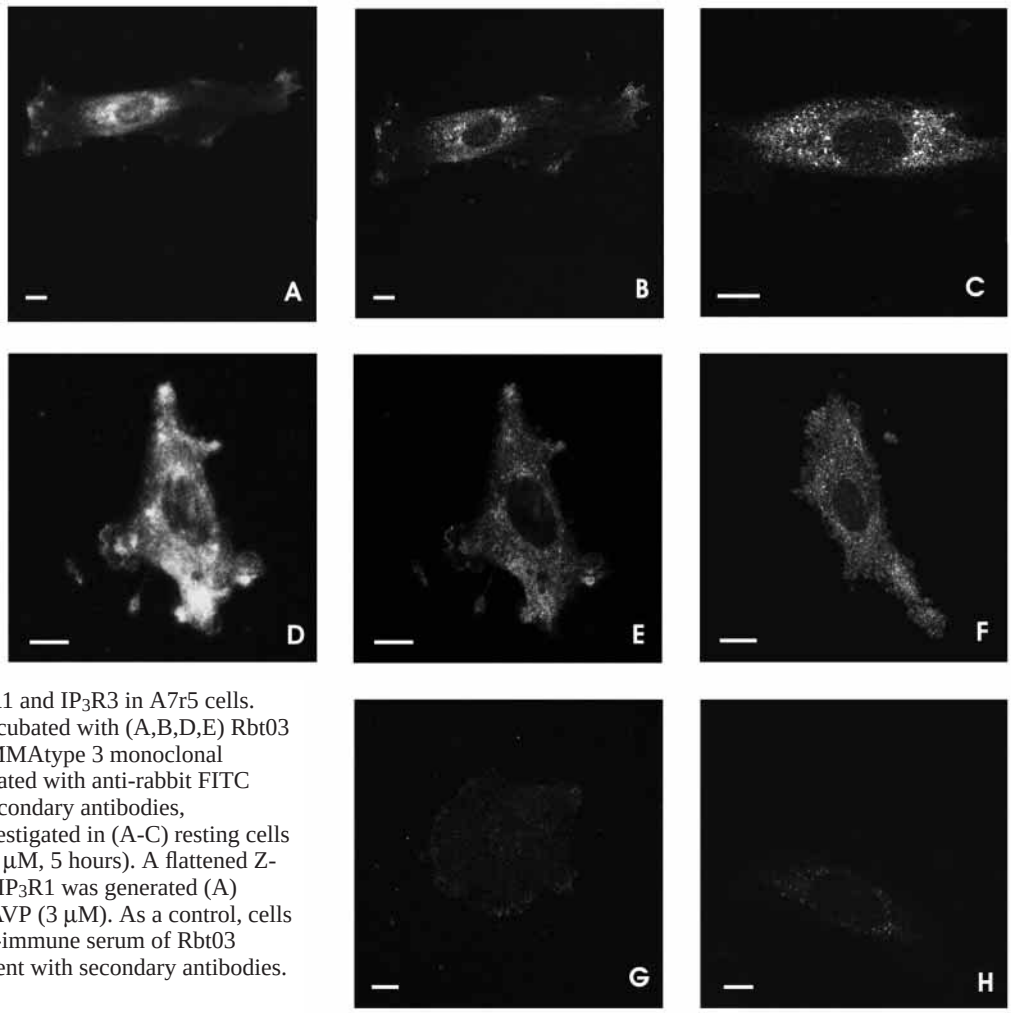

Fig. 1. Subcellular localization of IP_3R1 and IP_3R3 in A7r5 cells. Cells were fixed, permeabilized and incubated with (A,B,D,E) Rbt03 polyclonal antibody (1/750) or (C,F) MMAtype 3 monoclonal antibody (1/100), and subsequently treated with anti-rabbit FITC (1/750) or anti-mouse FITC (1/500) secondary antibodies, respectively. IP_3R localization was investigated in (A-C) resting cells or (D-F) after stimulation with AVP (3 μM, 5 hours). A flattened Z-stack image of the confocal images of IP_3R1 was generated (A) before and (D) after stimulation with AVP (3 μM). As a control, cells were incubated either (G) with the pre-immune serum of Rbt03 (1/750) or (H) with PBS before treatment with secondary antibodies. Bar, 10 μm.

containing transfected cells were investigated 18 hours after transfection with the Zeiss CLSM equipped with a Plan-Neofluar® 100x, numerical aperture 1.3 oil-immersion objective.

The microtubular network was visualized using the monoclonal antibody against α-tubulin (1/2000) as the primary antibody. As a control, cells were treated as above but incubated with PBS before the secondary antibody was added. Since preservation of the microtubular structure may be dependent on the fixation procedure, we also analyzed microtubuli after fixation in methanol (–20°C, 3 minutes). Finally, actin was visualized using rhodamine-phalloidin (1 unit/ml).

Statistics

Data are represented as means±s.e.m. and considered significantly different when $P<0.05$ by use of Student's unpaired *t*-test. "*n*" represents the number of independent experiments.

Results and Discussion

Intracellular localization of IP_3R1 and IP_3R3 in A7r5 cells

We used immunofluorescent labeling and confocal microscopy to visualize the IP_3Rs in A7r5 cells, which are known to express IP_3R1 and IP_3R3 (De Smedt et al., 1994). In these cells, IP_3R1 is the predominantly expressed isoform and appears to be functionally different from IP_3R3 (Missiaen et al., 1998; Wang et al., 2001). Moreover, IP_3R1 seems to be more important than IP_3R3, not only for IP_3-induced Ca^{2+} release but also for capacitative Ca^{2+} entry and proliferation (Wang et al., 2001). The localization of IP_3R1 was investigated using the Rbt03 antibody directed against the C-terminus of IP_3R1. In unstimulated cells, IP_3R1 was predominantly located in the perinuclear region resulting in a broad perinuclear ring-like structure. This was observed in a flattened Z-stack of the cell (Fig. 1A) and in single confocal images (Fig. 1B), showing that this distribution existed throughout the entire cell. A number of isolated patches of IP_3R1 were also detected near the periphery of the cells. Identical results were obtained with antibodies recognizing other epitopes of IP_3R1 (data not shown). In contrast, IP_3R3 displayed a more punctate staining pattern, homogeneously distributed over the entire cytoplasm (Fig. 1C).

Redistribution of IP_3R1 after prolonged AVP stimulation

It has already been shown that in neutrophils, cellular activation can affect the localization of the intracellular Ca^{2+} stores (Stendahl et al., 1994). Furthermore, short-term agonist stimulation can also lead to clustering of IP_3Rs (Wilson et al., 1998). Here we investigated the role of long-term agonist

stimulation on the localization of IP_3Rs in A7r5 cells. After prolonged stimulation of the cells (5 hours) with a supramaximal concentration of AVP (3 μM) and in the absence of extracellular Ca^{2+}, a dramatic change was observed in the intracellular localization of IP_3R1. A redistribution of IP_3R1 from the perinuclear region to a more uniform cytoplasmic distribution occurred (Fig. 1D,E), while no changes in the localization of IP_3R3 could be seen (Fig. 1F). Since the redistribution was also observed after the separate confocal images of the Z-stack were superimposed (Fig. 1D), it represents an overall change in localization. Background fluorescence was negligible for both isoforms as shown in Fig. 1G,H.

To quantify the level of redistribution of IP_3R1, we assessed the number of A7r5 cells with the IP_3R1 predominantly localized in the perinuclear region, or homogeneously distributed in the cytoplasm. When comparing control cells with cells pretreated for 5 hours with AVP (3 μM), the percentage of cells with a perinuclear IP_3R1 localization decreased from 74.3±3.2% (n=3) in control cells to 21.3±1.3% (n=3) in AVP-stimulated cells. Simultaneously, the percentage of cells with a cytoplasmic IP_3R1 distribution increased from 15.0±3.6% (n=3) in control cells to 72.7±2.3% (n=3) in AVP-stimulated cells. The number of cells in an intermediate state was similar in control cells and in cells stimulated with AVP (10.7±1.2% [n=3] and 6.0±2.5% [n=3], respectively). Identical observations were made in the presence of extracellular Ca^{2+} (1 mM), although the fluorescence signal was weaker, probably because of enhanced degradation of the IP_3Rs (data not shown). The redistribution of IP_3R1 was observed with Rbt03, as well as with other antibodies directed against the N- or the C-terminal part of IP_3R1, excluding the possibility that the redistribution process only affected a fragment of IP_3R1.

Because prolonged stimulation of cells is known to downregulate IP_3Rs (Wojcikiewicz et al., 1994) via the ubiquitin-proteasome pathway (Oberdorf et al., 1999), we also investigated the redistribution of IP_3Rs in the presence of the proteasome inhibitor MG-132. When added alone MG-132 (20 μM) affected the localization of IP_3R1 (only 49.5±0.5% [n=2] of the MG-132-treated cells had a perinuclear IP_3R1 localization). The AVP-induced redistribution, however, occurred to the same extent in the presence or absence of MG-132 (26.3±1.9% [n=3] of cells with a perinuclear localization).

Time dependence of IP_3R1 redistribution

To investigate the time course of the redistribution, we visualized IP_3R1 in cells incubated with AVP for various times. Fig. 2 shows the percentage of cells with a perinuclear or a homogeneous distribution of IP_3R1 as a function of time of incubation with AVP (3 μM). Interestingly, during the first hour, IP_3R1 remained localized in the perinuclear region. The redistribution occurred mainly during the second hour after AVP addition, after which it stabilized. We examined whether this process was reversible by removing AVP after 2 hours. Within one hour, there was a nearly full recovery of the original perinuclear distribution (dotted line in Fig. 2), indicating that cells suffered no irreversible damage. Identical results were obtained in the presence or absence of extracellular Ca^{2+}. These results provide further evidence that the redistribution occurs independently of downregulation, since downregulation

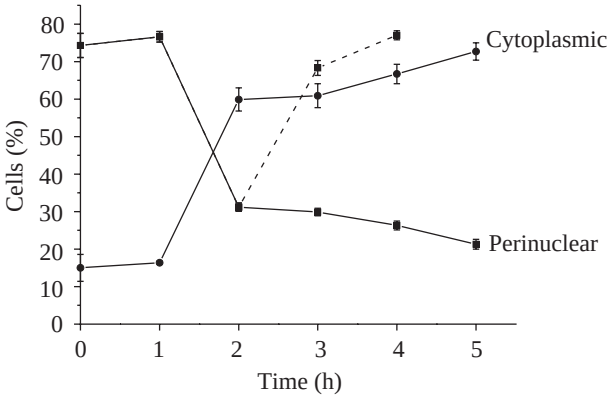

Fig. 2. Time course of IP_3R1 redistribution. The percentage of cells with IP_3R1 located in the perinuclear region (squares) and in the cytoplasm (circles) after addition of 3 μM AVP is depicted for different time periods. The dashed line represents the removal of AVP (3 μM) after 2 hours, after which the cells where incubated in PBS without Ca^{2+} for the indicated time periods. Each result is the mean±s.e.m. from three independent experiments. The s.e.m. is not indicated when smaller than the symbol.

was shown to be much slower and more gradual (Sipma et al., 1998). Moreover, downregulation is an irreversible process (Oberdorf et al., 1999), whereas the redistribution was fully reversible.

IP_3R1 redistribution can be induced by Ca^{2+}-releasing agents

In A7r5 cells, AVP stimulates a single class of vasopressin receptors (V_{1A}) leading to the activation of PLC, phospholipase D and phospholipase A_2. We used the PLC activator imipramine (Fukuda et al., 1994) to examine whether the inositol lipid signaling pathway was involved in IP_3R1 redistribution. Imipramine (50 μM) added to the cells for 4 hours was able to induce the redistribution as effectively as AVP (3 μM) for the same time period (with imipramine 20.0±7.0% [n=2] and with AVP 26.3±1.2% [n=3] of cells with IP_3R1 located in the perinuclear region) indicating that the inositol lipid signaling pathway is involved. Since PLC activation leads to the production of IP_3 and DAG, we investigated the role of each of these second messengers. Raising only the intracellular IP_3 concentration by using a cell permeable IP_3 ester (IP_3BM) (Thomas et al., 2000) induced the redistribution of IP_3R1 (data not shown). Furthermore, increasing the free cytoplasmic Ca^{2+} concentration by emptying the stores using the SERCA pump inhibitors thapsigargin and CPA also led to an identical redistribution of IP_3R1 (Fig. 3).

PKC is involved in the redistribution of IP_3R1

A common downstream target of DAG and Ca^{2+} is PKC. We therefore determined whether PKC could play a role in the redistribution of IP_3R1. Activation of PKC with 50 μM of the diacylglycerol analog OAG for 5 hours caused the redistribution of IP_3R1 to the cytoplasm, which was nearly as prominent as that obtained with AVP (Table 1). This result was verified by the use of different PKC inhibitors (Table 1).

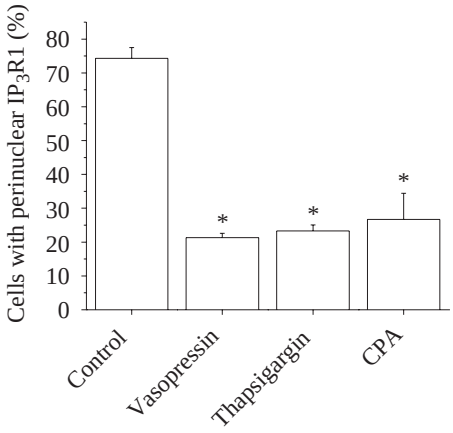

Fig. 3. Effect of Ca^{2+}-mobilizing agents on IP_3R1 redistribution. The percentage of cells with a perinuclear IP_3R1 is depicted before and after incubation with AVP (3 μM), thapsigargin (1 μM) and CPA (50 μM) for 5 hours. Each result is the mean±s.e.m. from three independent experiments. *Significantly different from the control.

Table 1. Effect of PKC activation and inhibition on the AVP- or thapsigargin-induced IP_3R1 redistribution

Condition	Perinucleary localized IP_3R1 (% of cells)
Control	74.3±3.1
AVP (3 μM)	21.3±1.3*
OAG (50 μM)	31.0±8.1*
Staurosporine (200 nM)	84.0±2.0
Staurosporine (200 nM) + AVP (3 μM)	75.7±4.5
Staurosporine (200 nM) + thapsigargin (1 μM)	78.7±3.5
Bisindolylmaleimide I hydrochloride (100 nM)	71.3±2.4
Bisindolylmaleimide I hydrochloride (100 nM) + AVP (3 μM)	52.7±0.9*
Gö-6976 (0.5 μM)	74.7±3.7
Gö-6976 (0.5 μM) + AVP (3 μM)	53.3±1.8*

A7r5 cells were incubated for 5 hours with the PKC activator OAG alone or with different PKC inhibitors in the presence of AVP (3 μM) or thapsigargin (1 μM). The percentages of cells with IP_3R1 localized in the perinuclear region are shown. Each result is the mean±s.e.m. from three independent experiments.

*Significantly different from the control.

Staurosporine (200 nM), a broad-spectrum inhibitor of protein kinases, inhibited both the AVP- and thapsigargin-induced redistribution. When added alone, it had no effect on the IP_3R1 localization. Staurosporine, however, did not change the cytoplasmic localization of IP_3R3, showing that the observed inhibition was not due to a general collapse of the ER structure around the nucleus (data not shown). The more selective PKC inhibitor bisindolylmaleimide I hydrochloride (100 nM) added to the cells together with AVP induced only a partial inhibition of the redistribution of IP_3R1, whereas the inhibitor itself had no effect on the intracellular localization of IP_3R1. Gö-6976, a specific inhibitor of the PKCα and PKCβ isoforms, also had no effect on the localization of IP_3R1 itself, but again partially inhibited the redistribution when added to the cells together with AVP. The partial inhibition of the redistribution by bisindolylmaleimide I hydrochloride and Gö-6976 may be explained by the fact that these compounds differently inhibit the various PKC isoforms. In A7r5 cells, three isoforms of PKC are activated upon stimulation with AVP, namely α, δ and ε (Fan and Byron, 2000). Staurosporine (200 nM) inhibits the α, β_I, β_{II}, γ, δ and ε isoforms, bisindolylmaleimide I hydrochloride the α, β_I, δ and ε isoform and Gö-6976 inhibits the α and β_I isoforms. Taking the effects of the various PKC inhibitors into account, our findings therefore strongly suggest a role for at least PKCα in the redistribution process.

Role of the microtubular network in IP_3R1 redistribution

Since PKC has been shown to modulate the cytoskeleton (Keenan and Kelleher, 1998), which has an important function in vesicle trafficking processes, we investigated whether microfilaments or microtubules were involved in IP_3R1 redistribution. Actin was visualized using rhodamine-phalloidin. In resting cells, the actin microfilaments appeared as stress fibers dispersed over the whole cell (Fig. 4B). Stimulation for 5 hours with AVP or OAG did not lead to significant structural changes (Fig. 4D,F).

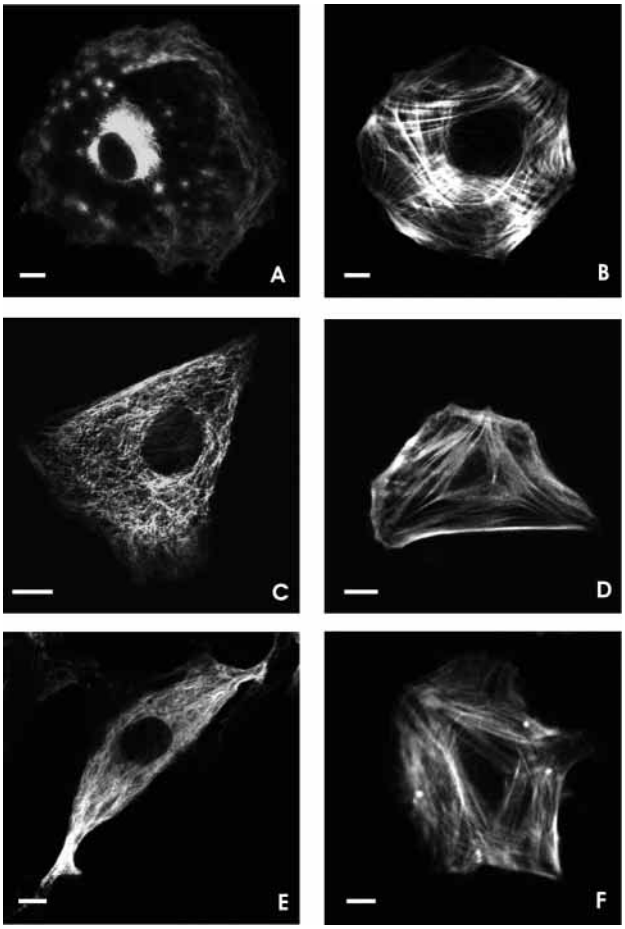

Fig. 4. Visualization of the microtubular and actin cytoskeleton. Cells were fixed, permeabilized and incubated (A,C,E) with anti-α tubulin (1/2000) or (B,D,F) with rhodamine-phalloidin (1 unit/ml). (A,C,E) Anti-mouse FITC (1/400) was used as secondary antibody. The microtubular and actin cytoskeleton was visualized (A,B) before and after (C,D) AVP (3 μM) or (E,F) OAG (50 μM) treatment for 5 hours. Bar, 10 μm.

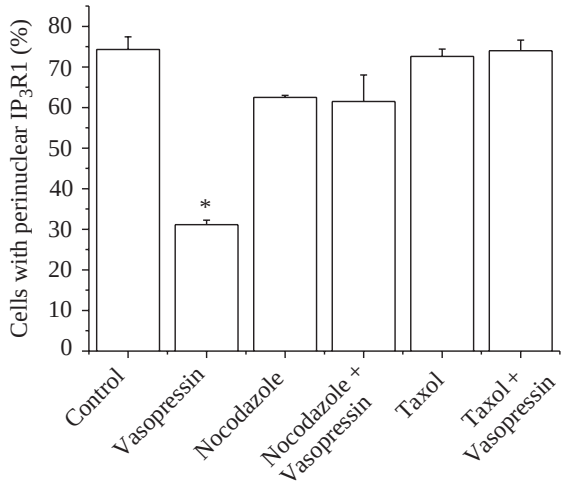

Fig. 5. Effect of nocodazole and taxol on IP_3R1 redistribution. The percentage of cells with a perinuclear IP_3R1 distribution is shown after incubation with AVP (3 μM) for 2 hours in the absence or presence of nocodazole (50 μM) or in the absence or presence of taxol (1 μM). Each result is the mean±s.e.m. from three independent experiments. *Significantly different from the control.

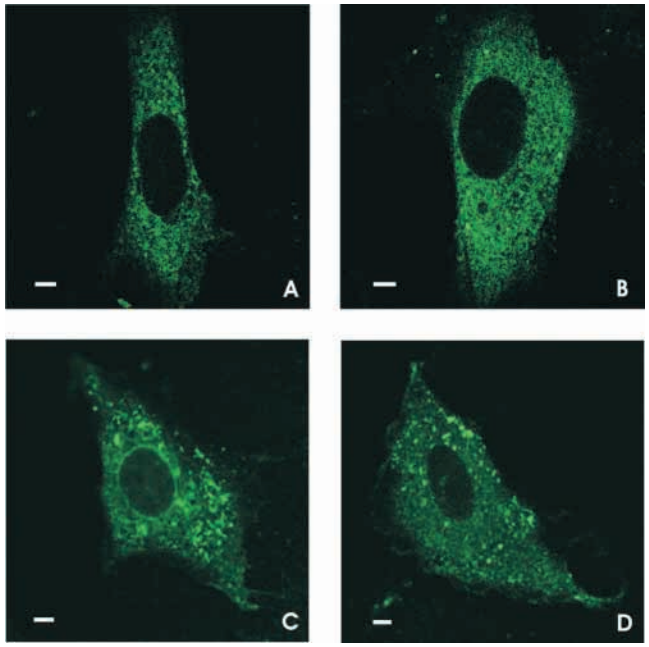

Fig. 6. Endoplasmic reticulum structure of A7r5 cells. ER structure was visualized in cells transfected with the pEYFP-ER vector, which encodes an ER-targeted yellow fluorescent fusion protein. The general ER morphology of (A) unstimulated and (B) AVP (3 μM, 5 hours) stimulated cells did not show significant differences. PDI was visualized (C) before and (D) after stimulation with AVP (3 μM, 2 hours) using the monoclonal anti-PDI antibody (1/100) and anti-mouse FITC (1/750). Bar, 5 μm.

Microtubules were visualized using an antibody directed against α-tubulin. In unstimulated A7r5 cells, the microtubular network consisted of short tubules, which were predominantly found around the nucleus, and long tubules located under the plasma membrane as can be seen in Fig. 4A. After 5 hours of stimulation with AVP (3 μM), the microtubules had spread out over the entire cytoplasm (Fig. 4C). Identical results were obtained when PKC was activated with OAG for 5 hours (Fig. 4E). Visualizing the microtubules after fixation with methanol gave similar results (data not shown), although quantitatively some differences were observed. In particular, although in paraformaldehyde-treated cells about 80% of the cells were characterized by a tubular network concentrated around the nucleus, such a pattern was only detected unambiguously in about 30% of the cells after methanol fixation. This pattern was, however, seldom found after AVP or OAG treatment, and this was independent of the fixation technique. PKC has already been shown to affect the microtubules. In neuronal growth cones, activation of PKC increased the growth lifetime of the microtubules, thereby promoting the extension of the distal microtubules from the central domain into the F-actin-rich peripheral domain where they are normally excluded (Kabir et al., 2001).

To further investigate the potential role of the microtubules in the redistribution process, we used the microtubule-disrupting agent nocodazole and the microtubule-stabilizing agent taxol. Fig. 5 shows the number of cells that contained a perinuclear IP_3R1 distribution after 2 hours of stimulation with AVP (3 μM) in the absence or presence of nocodazole (50 μM) or taxol (1 μM). The results show that both nocodazole and taxol could completely inhibit the AVP-induced redistribution, while each agent itself had no effect on the perinuclear localization of IP_3R1 (Fig. 5). Interestingly, neither compound affected the localization of IP_3R3 (data not shown). Taken together, these results clearly indicate an important role for the microtubular network in IP_3R1 redistribution.

Specific ER proteins redistribute after AVP stimulation

ER structure is known to be susceptible to changes in physiological situations such as oocyte maturation (Terasaki et al., 2001) or after prolonged increases in cytosolic Ca^{2+} concentration (Subramanian and Meyer, 1997). In addition, it was shown that PKC could protect the structure of the ER from the effects of abnormally high cytosolic Ca^{2+} concentrations (Ribeiro et al., 2000). Since the IP_3R is mainly an ER-residing protein, we first verified whether the gross morphology of the ER was modified after agonist stimulation. To visualize the ER structure, cells were transfected with the pEYFP-ER vector, which encodes an ER-targeted yellow fluorescent fusion protein. The effect of prolonged incubation with AVP on ER structure was examined 18 hours after transfection. Confocal images of paraformaldehyde-fixed cells were obtained from control cells and from cells treated with AVP (3 μM) for 5 hours. Fig. 6A shows a representative control cell. The ER appeared as an intricate network of tubules and vesicular structures expanding from the nuclear envelope to the periphery of the cell. Incubation of cells for 5 hours with AVP did not lead to significant changes in ER morphology (Fig. 6B). To avoid possible fixation artifacts, identical experiments were performed on intact cells, with similar results (data not shown).

Furthermore, we investigated whether typical ER-residing proteins displayed a similar behavior as IP_3R1. PDI was homogeneously distributed over the entire cell, both in unstimulated and AVP-stimulated cells (Fig. 6C,D). Staining patterns for the chaperone protein BiP were identical to those

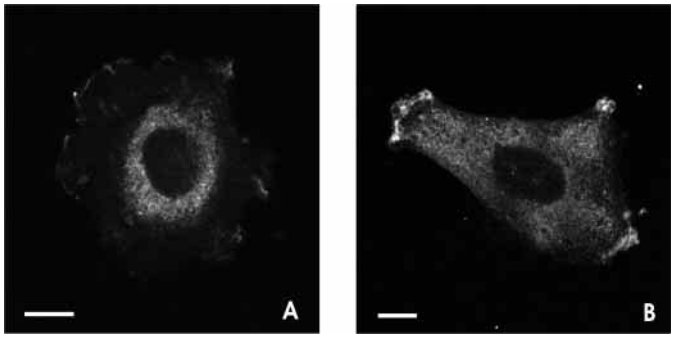

Fig. 7. Visualization of SERCA pumps in A7r5. Cells were fixed, permeabilized and incubated with AS809-27 polyclonal antibody (1/300). Anti-rabbit FITC (1/750) was used as secondary antibody. SERCA was visualized in (A) resting cells and (B) after stimulation with AVP (3 μM, 2 hours). Bar, 10 μm.

of PDI and are consistent with ER structure staining (data not shown).

Finally, we investigated the localization of the SERCA-type Ca^{2+} pumps. These pumps are important for the filling of the Ca^{2+} stores, and are thought to functionally co-localize with the Ca^{2+} release channels (Favre et al., 1996). Interestingly, in unstimulated cells SERCA distribution was similar to IP_3R1 distribution, i.e. predominantly found in the perinuclear region, although to a lesser extent (51.0±1.2% [*n*=3] of cells with perinuclear SERCA compared with 74.3±3.2% [*n*=3] of cells with perinuclear IP_3R1) (Fig. 7A). In addition, isolated peripheral patches were also found for SERCA. After stimulation with AVP (3 μM) for 2 hours, a redistribution of SERCA occurred from the perinuclear region to a more homogeneous distribution over the entire cell (33.0±1.0% [*n*=3] of cells with a perinuclear SERCA) (Fig. 7B). These results indicate that although the general ER structure is not affected, specific proteins involved in Ca^{2+} signaling processes, such as IP_3R1 and SERCA, are redistributed after prolonged agonist stimulation.

Potential role of vesicle trafficking in IP_3R1 redistribution

Although the ER can be considered as one continuous membrane compartment, the subcellular localization of intracellular Ca^{2+} release channels located to the ER may not be uniform (Petersen et al., 2001). In A7r5 cells, it has been shown that the perinuclear region functionally contained the highest density of Ca^{2+} stores (Blatter, 1995). In resting A7r5 cells, IP_3R1 is precisely concentrated in that region. In some cell types, it was shown that IP_3R1 localization could be restricted by its interaction with scaffolding proteins such as homer (Tu et al., 1998; Salanova et al., 2002) or ankyrin-B (Mohler et al., 2002). A restricted localization by interaction with cytoskeletal proteins could also be responsible for IP_3R1 localized at the cell periphery (Sugiyama et al., 2000). Prolonged cellular activation might modulate these interactions and could result in the unrestricted movement of IP_3Rs within the structure of the ER. Results obtained thus far, however, do not point to a significant role of homer or ankyrin in IP_3R distribution in A7r5 cells (E. Venmans, E.V., H.D.S. and J.B.P., unpublished).

Another possibility is that IP_3R1 is located in the perinuclear region and redistributes to the ER through vesicle trafficking. To investigate this hypothesis we first verified whether brefeldin A could affect IP_3R1 localization. Brefeldin A (2 μg/ml) treatment for 2 hours induced a complete redistribution of IP_3R1 (after treatment: 29.3±1.7% [*n*=4] cells with a predominant perinuclear localization), suggesting that vesicle trafficking might be involved.

Because the perinuclear immunostainings of IP_3R1 in resting cells are suggestive of IP_3R1 being localized in the vesiculotubular clusters of the intermediate compartment, we incubated cells for 2 hours at 15°C. At this temperature, the vesicular transport of proteins is blocked at the level of the intermediate compartment (Saraste and Kuismanen, 1984). Such treatment had no effect on the localization of the IP_3R1 (71.3±3.5% [*n*=3] of cells with a perinuclear localization of IP_3R1) but completely inhibited its AVP-induced redistribution (after treatment 75.7±2.6% [*n*=3] of cells with a perinuclear localization of IP_3R1). Similar results were obtained when thapsigargin was applied to induce the redistribution.

These results strongly suggest a role for vesicle trafficking in the redistribution process. Moreover, our results concerning the AVP-induced redistribution of the SERCA pumps are in good agreement with this hypothesis. Indeed, it might be expected that IP_3R1 and SERCA redistribution are related. Although both Ca^{2+} transport proteins functionally co-localize (Favre et al., 1996), there is no evidence for either a direct or an indirect structural interaction between both. Finally, the results obtained in the presence of nocodazole or taxol indicate that the microtubular network, which is known to play an important role in vesicular trafficking, is likely to be involved in the redistribution. These results are in agreement with recent results describing that the redistribution of the Ca^{2+} stores in newt eggs also required the microtubular network (Mitsuyama and Sawai, 2001). Moreover, PKC that also activates IP_3R1 redistribution is related to microtubular outgrowth (Kabir et al., 2001) and to ER organization after excessive Ca^{2+} release (Ribeiro et al., 2000).

Conclusion

In conclusion, our work indicates that prolonged agonist stimulation can lead to a redistribution of specific proteins involved in Ca^{2+} signaling. In A7r5 smooth muscle cells, the redistribution affected IP_3R1 and the SERCA pumps. This redistribution process depends on PKC activity and on the integrity of the microtubular network and probably involves vesicle trafficking. The redistribution of Ca^{2+}-store elements might represent an adaptive response of the cell to prolonged cellular activation.

We thank Irène Willems, Marina Crabbé, Luce Heremans, Jerry Renders, Yves Parijs, Anja Florizoone and Lea Bauwens for their skillful technical assistance. We acknowledge the generous gift of IP_3BM by M. D. Bootman (Babraham, UK), of the AS809-27 antibody by J. V. Møller (University of Aarhus, Denmark), and the assistance in the production of the anti-loopI17a-2 and anti-cytI3b-1 antibodies by I. Sienaert. We thank M. Opas and S. Papp (University of Toronto) and P. S. McPherson (McGill University) for stimulating discussions. This work was supported in part by Grant 99/08 of the Concerted Actions of the K. U. Leuven.

References

Berridge, M. J. (1993). Inositol trisphosphate and calcium signalling. *Nature* **361**, 315-325.

Berridge, M. J., Bootman, M. D. and Lipp, P. (1998). Calcium, a life and death signal. *Nature* **395**, 645-648.

Blatter, L. A. (1995). Depletion and filling of intracellular calcium stores in vascular smooth muscle. *Am. J. Physiol.* **268**, C503-512.

Bootman, M. D. and Berridge, M. J. (1995). The elemental principles of calcium signaling. *Cell* **83**, 675-678.

De Smedt, H., Missiaen, L., Parys, J. B., Bootman, M. D., Mertens, L., Van den Bosch, L. and Casteels, R. (1994). Determination of relative amounts of inositol trisphosphate receptor mRNA isoforms by ratio polymerase chain reaction. *J. Biol. Chem.* **269**, 21691-21698.

De Smedt, H., Missiaen, L., Parys, J. B., Henning, R. H., Sienaert, I., Vanlingen, S., Gijsens, A., Himpens, B. and Casteels, R. (1997). Isoform diversity of the inositol trisphosphate receptor in cell types of mouse origin. *Biochem. J.* **322**, 575-583.

Fan, J. and Byron, K. L. (2000). Ca^{2+} signalling in rat vascular smooth muscle cells: a role for protein kinase C at physiological vasoconstrictor concentrations of vasopressin. *J. Physiol.* **524**, 821-831.

Favre, C. J., Jerstrom, P., Foti, M., Stendhal, O., Huggler, E., Lew, D. P. and Krause, K. H. (1996). Organization of Ca^{2+} stores in myeloid cells: association of SERCA2b and the type-1 inositol-1,4,5-trisphosphate receptor. *Biochem. J.* **316**, 137-142.

Fissore, R. A., Longo, F. J., Anderson, E., Parys, J. B. and Ducibella, T. (1999). Differential distribution of inositol trisphosphate receptor isoforms in mouse oocytes. *Biol. Reprod.* **60**, 49-57.

Fogarty, K. E., Kidd, J. F., Turner, A., Skepper, J. N., Carmichael, J. and Thorn, P. (2000). Microtubules regulate local Ca^{2+} spiking in secretory epithelial cells. *J. Biol. Chem.* **275**, 22487-22494.

Fukuda, H., Nishida, A., Saito, H., Shimizu, M. and Yamawaki, S. (1994). Imipramine stimulates phospholipase C activity in rat brain. *Neurochem. Int.* **25**, 567-571.

Hirata, K., Nathanson, M. H., Burgstahler, A. D., Okazaki, K., Mattei, E. and Sears, M. L. (1999). Relationship between inositol 1,4,5-trisphosphate receptor isoforms and subcellular Ca^{2+} signaling patterns in nonpigmented ciliary epithelia. *Invest. Ophthalmol. Vis. Sci.* **40**, 2046-2053.

Kabir, N., Schaefer, A. W., Nakhost, A., Sossin, W. S. and Forscher, P. (2001). Protein kinase C activation promotes microtubule advance in neuronal growth cones by increasing average microtubule growth lifetimes. *J. Cell Biol.* **152**, 1033-1044.

Keenan, C. and Kelleher, D. (1998). Protein kinase C and the cytoskeleton. *Cell Signal* **10**, 225-232.

Laflamme, K., Domingue, O., Guillemette, B. I. and Guillemette, G. (2002). Immunohistochemical localization of type 2 inositol 1,4,5-trisphosphate receptor to the nucleus of different mammalian cells. *J. Cell. Biochem.* **85**, 219-228.

Lee, M. G., Xu, X., Zeng, W., Diaz, J., Wojcikiewicz, R. J., Kuo, T. H., Wuytack, F., Raeymaekers, L. and Muallem, S. (1997). Polarized expression of Ca^{2+} channels in pancreatic and salivary gland cells. Correlation with initiation and propagation of $[Ca^{2+}]_i$ waves. *J. Biol. Chem.* **272**, 15765-15770.

Maes, K., Missiaen, L., Parys, J. B., De Smet, P., Sienaert, I., Waelkens, E., Callewaert, G. and De Smedt, H. (2001). Mapping of the ATP-binding sites on inositol 1,4,5-trisphosphate receptor type 1 and type 3 homotetramers by controlled proteolysis and photoaffinity labeling. *J. Biol. Chem.* **276**, 3492-3497.

Marchant, J. S. and Parker, I. (2001). Role of elementary Ca^{2+} puffs in generating repetitive Ca^{2+} oscillations. *EMBO J.* **20**, 65-76.

Missiaen, L., De Smedt, H., Parys, J. B., Sienaert, I., Vanlingen, S. and Casteels, R. (1996). Threshold for inositol 1,4,5-trisphosphate action. *J. Biol. Chem.* **271**, 12287-12293.

Missiaen, L., Parys, J. B., Sienaert, I., Maes, K., Kunzelmann, K., Takahashi, M., Tanzawa, K. and De Smedt, H. (1998). Functional properties of the type-3 $InsP_3$ receptor in 16HBE14o-bronchial mucosal cells. *J. Biol. Chem.* **273**, 8983-8986.

Mitsuyama, F. and Sawai, T. (2001). The redistribution of Ca^{2+} stores with inositol 1,4,5-trisphosphate receptor to the cleavage furrow in a microtubule-dependent manner. *Int. J. Dev. Biol.* **45**, 861-868.

Mohler, P. J., Gramolini, A. O. and Bennett, V. (2002). The ankyrin-B C-terminal domain determines activity of ankyrin-B/G chimeras in rescue of abnormal inositol 1,4,5-trisphosphate and ryanodine receptor distribution in ankyrin-B (–/–) neonatal cardiomyocytes. *J. Biol. Chem.* **277**, 10599-10607.

Møller, J. V., Ning, G., Maunsbach, A. B., Fujimoto, K., Asai, K., Juul, B., Lee, Y. J., Gomez de Gracia, A., Falson, P. and le Maire, M. (1997). Probing of the membrane topology of sarcoplasmic reticulum Ca^{2+}-ATPase with sequence-specific antibodies. Evidence for plasticity of the C- terminal domain. *J. Biol. Chem.* **272**, 29015-29032

Nelson, M. T., Cheng, H., Rubart, M., Santana, L. F., Bonev, A. D., Knot, H. J. and Lederer, W. J. (1995). Relaxation of arterial smooth muscle by calcium sparks. *Science* **270**, 633-637.

Nishizuka, Y. (1988). The molecular heterogeneity of protein kinase C and its implications for cellular regulation. *Nature* **334**, 661-665.

Oberdorf, J., Webster, J. M., Zhu, C. C., Luo, S. G. and Wojcikiewicz, R. J. (1999). Down-regulation of types I, II and III inositol 1,4,5-trisphosphate receptors is mediated by the ubiquitin/proteasome pathway. *Biochem. J.* **339**, 453-461.

Parys, J. B., De Smedt, H., Missiaen, L., Bootman, M. D., Sienaert, I. and Casteels, R. (1995). Rat basophilic leukemia cells as model system for inositol 1,4,5-trisphosphate receptor IV, a receptor of the type II family: functional comparison and immunological detection. *Cell Calcium* **17**, 239-249.

Patel, S., Joseph, S. K. and Thomas, A. P. (1999). Molecular properties of inositol 1,4,5-trisphosphate receptors. *Cell Calcium* **25**, 247-264.

Petersen, O. H., Tepikin, A. and Park, M. K. (2001). The endoplasmic reticulum: one continuous or several separate Ca^{2+} stores? *Trends Neurosci.* **24**, 271-276.

Powell, J. A., Carrasco, M. A., Adams, D. S., Drouet, B., Rios, J., Muller, M., Estrada, M. and Jaimovich, E. (2001). IP_3 receptor function and localization in myotubes: an unexplored Ca^{2+} signaling pathway in skeletal muscle. *J. Cell Sci.* **114**, 3673-3683.

Ribeiro, C. M. P., McKay, R. R., Hosoki, E., Bird, G. S. and Putney, J. W. (2000). Effects of elevated cytoplasmic calcium and protein kinase C on endoplasmic reticulum structure and function in HEK293 cells. *Cell Calcium* **27**, 175-185.

Salanova, M., Priori, G., Barone, V., Intravaia, E., Flucher, B., Ciruela, F., McIlhinney, R. A., Parys, J. B., Mikoshiba, K. and Sorrentino, V. (2002). Homer proteins and $InsP_3$ receptors co-localise in the longitudinal sarcoplasmic reticulum of skeletal muscle fibres. *Cell Calcium* **32**, 193-200.

Saraste, J. and Kuismanen, E. (1984). Pre- and post-Golgi vacuoles operate in the transport of Semliki Forest virus membrane glycoproteins to the cell surface. *Cell* **38**, 535-549.

Sipma, H., Deelman, L., De Smedt, H., Missiaen, L., Parys, J. B., Vanlingen, S., Henning, R. H. and Casteels, R. (1998). Agonist-induced down-regulation of type 1 and type 3 inositol 1,4,5-trisphosphate receptors in A7r5 and DDT1 MF-2 smooth muscle cells. *Cell Calcium* **23**, 11-21.

Sipma, H., De Smet, P., Sienaert, I., Vanlingen, S., Missiaen, L., Parys, J. B. and De Smedt, H. (1999). Modulation of inositol 1,4,5-trisphosphate binding to the recombinant ligand-binding site of the type-1 inositol 1,4,5-trisphosphate receptor by Ca^{2+} and calmodulin. *J. Biol. Chem.* **274**, 12157-12162.

Stendahl, O., Krause, K. H., Krischer, J., Jerstrom, P., Theler, J. M., Clark, R. A., Carpentier, J. L. and Lew, D. P. (1994). Redistribution of intracellular Ca^{2+} stores during phagocytosis in human neutrophils. *Science* **265**, 1439-1441.

Subramanian, K. and Meyer, T. (1997). Calcium-induced restructuring of nuclear envelope and endoplasmic reticulum calcium stores. *Cell* **89**, 963-971.

Sugiyama, T., Matsuda, Y. and Mikoshiba, K. (2000). Inositol 1,4,5-trisphosphate receptor associated with focal contact cytoskeletal proteins. *FEBS Lett.* **466**, 29-34.

Tasker, P. N., Taylor, C. W. and Nixon, G. F. (2000). Expression and distribution of $InsP_3$ receptor subtypes in proliferating vascular smooth muscle cells. *Biochem. Biophys. Res. Commun.* **273**, 907-912.

Terasaki, M., Runft, L. L. and Hand, A. R. (2001). Changes in organization of the endoplasmic reticulum during Xenopus oocyte maturation and activation. *Mol. Biol. Cell* **12**, 1103-1116.

Thomas, D., Lipp, P., Tovey, S. C., Berridge, M. J., Li, W., Tsien, R. Y. and Bootman, M. D. (2000). Microscopic properties of elementary Ca^{2+} release sites in non-excitable cells. *Curr. Biol.* **10**, 8-15.

Tu, J. C., Xiao, B., Yuan, J. P., Lanahan, A. A., Leoffert, K., Li, M., Linden, D. J. and Worley, P. F. (1998). Homer binds a novel proline-rich motif and links group 1 metabotropic glutamate receptors with IP_3 receptors. *Neuron* **21**, 717-726.

Van Acker, K., Bautmans, B., Bultynck, G., Maes, K., Weidema, A. F., De Smet, P., Parys, J. B., De Smedt, H., Missiaen, L. and Callewaert, G. (2000). Mapping of IP_3-mediated Ca^{2+} signals in single human

neuroblastoma SH-SY5Y cells: cell volume shaping the Ca^{2+} signal. *J. Neurophysiol.* **83**, 1052-1057.

Wang, Y., Chen, J., Taylor, C. W., Hirata, Y., Hagiwara, H., Mikoshiba, K., Toyo-oka, T., Omata, M. and Sakaki, Y. (2001). Crucial role of type 1, but not type 3, inositol 1,4,5-trisphosphate (IP_3) receptors in IP_3-induced Ca^{2+} release, capacitative Ca^{2+} entry, and proliferation of A7r5 vascular smooth muscle cells. *Circ. Res.* **88**, 202-209.

Wilson, B. S., Pfeiffer, J. R., Smith, A. J., Oliver, J. M., Oberdorf, J. A. and Wojcikiewicz, R. J. (1998). Calcium-dependent clustering of inositol 1,4,5-trisphosphate receptors. *Mol. Biol. Cell* **9**, 1465-1478.

Wojcikiewicz, R. J. (1995). Type I, II, and III inositol 1,4,5-trisphosphate receptors are unequally susceptible to down-regulation and are expressed in markedly different proportions in different cell types. *J. Biol. Chem.* **270**, 11678-11683.

Wojcikiewicz, R. J., Furuichi, T., Nakade, S., Mikoshiba, K. and Nahorski, S. R. (1994). Muscarinic receptor activation down-regulates the type I inositol 1,4,5-trisphosphate receptor by accelerating its degradation. *J. Biol. Chem.* **269**, 7963-7969.

Zhang, X., Wen, J., Bidasee, K. R., Besch, H. R., Jr, Wojcikiewicz, R. J., Lee, B. and Rubin, R. P. (1999). Ryanodine and inositol trisphosphate receptors are differentially distributed and expressed in rat parotid gland. *Biochem. J.* **340**, 519-527.